ECS Solid State Letters, **1** (6) Q57-Q60 (2012)
2162-8742/2012/1(6)/Q57/4/$28.00 © The Electrochemical Society

Fabrication and Characterization of $Li_7La_3Zr_2O_{12}$ Thin Films for Lithium Ion Battery

Jiajia Tan and Ashutosh Tiwari[z]

Nanostructured Materials Research Laboratory, Department of Materials Science and Engineering, University of Utah, Salt Lake City Utah, 84112, USA

Thin films of $Li_7La_3Zr_2O_{12}$ were deposited on $SrTiO_3$ (100) and Sapphire (0001) substrates at room-temperature using a pulsed-laser-deposition technique. Detailed structural, compositional, optical, and electrochemical characterizations of the films were performed. The films deposited at room-temperature had amorphous structure, and exhibited a lithium-ion conductivity of 3.35×10^{-7} S/cm. The effects of thermal annealing and pulsed laser annealing on the properties of the films were investigated. Pulsed laser annealed films were found to have a superior lithium-ion conductivity value of 7.36×10^{-7} S/cm. Moreover, the $Li_7La_3Zr_2O_{12}$ films were found to be electrochemically stable against lithium metal.
 [DOI: 10.1149/2.013206ssl]

Manuscript submitted June 6, 2012; revised manuscript received September 4, 2012. Published October 3, 2012.

The last few decades have seen a drastic miniaturization of electronic devices following the famous Moore's law predicted by Gordan Moore in 1971. These developments in the electronic industry have resulted in ultra-low-weight electronic devices such as palm-top computers, smart phones, tablet PCs etc. Batteries constitute one of the most important and essential components of these devices. At present, lithium ion batteries (LIBs) are considered the most suitable candidate for use in portable electronic devices. However, these batteries are available only in the bulk form and comprise a significant percentage of the overall weight of the device. As the miniaturization of electronic devices continues, we need more advanced batteries which are light weight, safe, and environment friendly. One possible solution is the development of thin film batteries (TFBs) which can be integrated onto the microprocessor chips themselves. For these applications, we would require solid-state (SS) electrolyte. Currently, a major obstacle in this field is the low ionic conductivity of SS electrolytes and high temperature needed to fabricate thin films of these materials.

As far as the research in SS electrolyte materials is concerned, many different kinds of inorganic systems have been explored to date. These include Nasicon-type electrolytes,[1–4] perovskite-type lithium lanthanum tantantes,[5,6] and garnet-type Li ion conductors.[7,8] Among all of them, garnet type $Li_7La_3Zr_2O_{12}$ (LLZO), synthesized lately by Weppner's group[9] has been reported to possess very high ionic conductivity. What's more, LLZO is electrochemically stable with a potential window wider than 0–7 V, is environment friendly, and is relatively inexpensive.[9–11] However, to our knowledge, LLZO has so far been synthesized in bulk form only; no work has been reported on the preparation of LLZO thin films. For realizing thin film batteries, it is essential to be able to grow thin films of solid electrolytes and preferably at low temperatures. In this paper, we are reporting the fabrication of LLZO thin films on $SrTiO_3$ (100) and Sapphire (0001) substrates by pulsed laser deposition at room temperature. The effect of annealing was investigated by detailed characterization of thin film structures and properties. Studies were also performed to understand the influence of lithium loss during the deposition process.

Experimental

A high purity LLZO target was synthesized by a solution-based technique. Stoichiometric amounts of Li_2CO_3, La_2O_3 and $ZrO(NO_3)_2 \cdot 6H_2O$ powders were dissolved in nitric acid and mixed with a chelating agent (citric acid). The solution was refluxed for 1 hour and concentrated to gel before drying into powders. The obtained powders were heated in flowing oxygen at 1230°C for 24 hrs.[12] In order to compensate lithium loss during laser deposition, a Li_2O target was prepared by sintering high purity Li_2O powders at 750°C for 8 hrs in flowing oxygen. A pulsed laser deposition (PLD) system equipped with a KrF excimer laser (248 nm wavelength and 25 ns pulse width) was employed for the depositions. Both the LLZO and the Li_2O targets were introduced into the PLD chamber. The laser pulse frequency was set to 10 Hz and the energy fluence was kept at 7.5 J/cm^2. The targets were ablated by the laser beam incident at an angle of 45°; the generated plume was deposited onto the substrates which were 4.5 cm away from the target. For every 100 shots of laser incident on LLZO target, 10 shots were made incident on Li_2O. A total of 7,700 shots were used for the deposition which resulted in a film thickness of approximately 1μm. The oxygen pressure in the chamber was varied from 10^{-3} mbar to 0.8 mbar, with 0.4 mbar found to be the most suitable value for achieving films of good stoichiometry. The films were post-annealed at different temperatures ranging from 600°C up to 1000°C for 30 min at a ramp rate of 5°C/min.

The crystal structure of the films was characterized by X-ray diffraction (XRD) technique using CuKα radiation ($\lambda = 1.54$ Å). The film morphology was analyzed by scanning electron microscopy (SEM). The measurement of electrical properties was conducted from room temperature to 60°C using the electrochemical impedance spectroscopy (EIS) function of a Gamry 600. For this, a Au/LLZO/Pt cell was fabricated by depositing Pt electrode on the surface of STO followed by the deposition of the LLZO film and then Au electrode on the top. The cell was heated at 80°C for 1 h before testing to ensure good electrical contact. The electrochemical stability of the films was tested on Li/LLZO/Pt/STO cells by cyclic voltammetry (CV) function of Gamry 600 from −0.5 V to 5 V at a scanning rate of 10 mV/s. The chemical composition of the films was analyzed by energy dispersive X-ray spectroscopy (EDS) and inductively coupled plasma mass spectrometry (ICP-MS). The optical properties of the films deposited on sapphire were tested using UV-VIS spectrometer, in the wavelength range of 190 nm to 1100 nm.

Results and Discussion

The XRD patterns of the as-deposited and annealed films grown on STO (100) substrates are shown in Figure 1a. The as-deposited films were amorphous, exhibiting no diffraction peak besides those of the substrate. Upon annealing at 800°C for 30 minutes, there appeared two broad peaks, which became sharper after further annealing at 1000°C for 30 minutes, indicating better crystallinity. In the films annealed at a1000°C, apart from the above two broad peaks few more peaks appeared and all of them were found to correspond to the crystal structure of cubic phase LLZO [JCPDS card reference code: 00-045-0109]. Here we noted that our films might be slightly textured in the ⟨100⟩ orientation, because the (400) peak was found to be the strongest in these films (see Figure 1b), instead of (420) which is the 100% peak in LLZO bulk system. It is worth noting that in bulk systems, at room temperature, cubic phase of LLZO is achievable only when doped by aluminum, tantalum or other elements.[13–15] The preservation of cubic phase of LLZO in our films could be attributed to lithium vacancies formed easily in the films during sintering, which

[z]E-mail: tiwari@eng.utah.edu

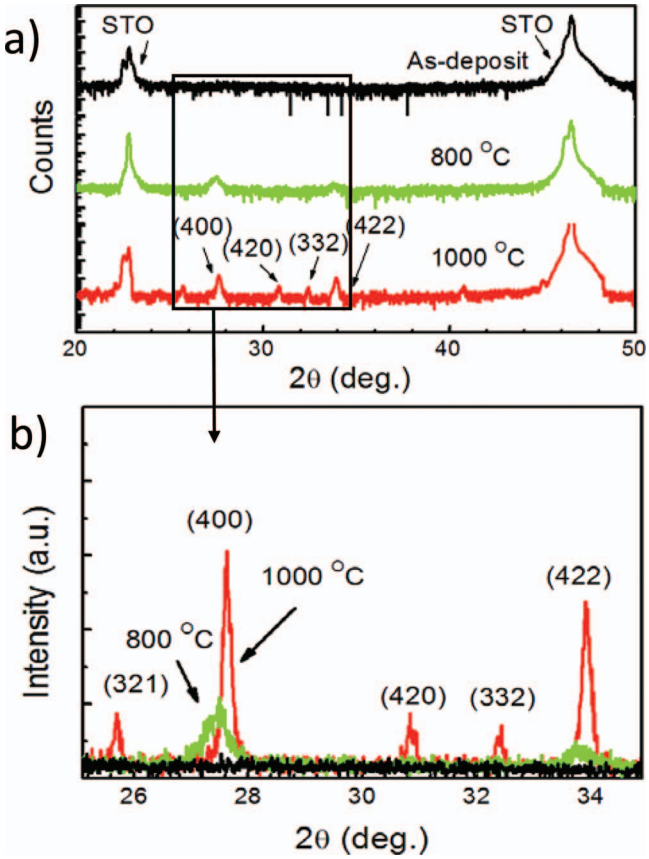

Figure 1. (a) XRD patterns of the as deposited and annealed films; (b) the magnified view.

increased the disorder of the lithium sites, thereby stabilizing the cubic phase at room temperature.

The surface morphology of the as-deposited films was found to be quite smooth as seen in the SEM image in Figure 2a. The scattered dots on top of the films can be reduced by lowering the laser energy or elongating the target-to-substrate distance. Figure 2b shows the surface of the films after sintering at 1000°C. Because of different thermal expansion coefficients between the film and the substrate or between different crystal orientations, a lot of cracks were formed. EDS measurements showed that the ratio of lanthanum and zirconium in the films was very close to the stoichiometric ratio of 3:2. These measurements were performed only on the films grown on sapphire (0001) substrate because Sr (which is a part of STO substrate) has overlapping characteristic X-ray peaks with Zr. Since Li cannot be detected by EDS we also performed ICP-MS measurements which confirmed the stoichiometric nature of the films prepared by our approach of using compensating Li_2O target.

The optical transmission spectra of the LLZO films deposited on sapphire (0001) substrates (as-deposited and as well as annealed) are

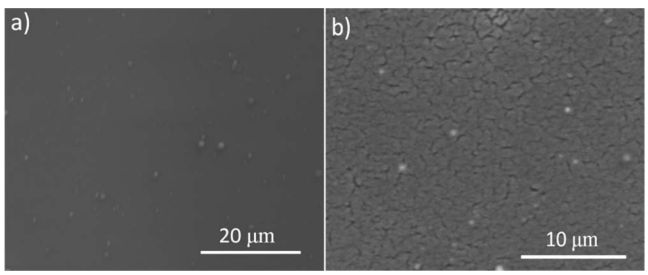

Figure 2. (a) Plane-view SEM image of the as-deposited LLZO film grown on STO (100), (b) Plane-view SEM image of the annealed LLZO film.

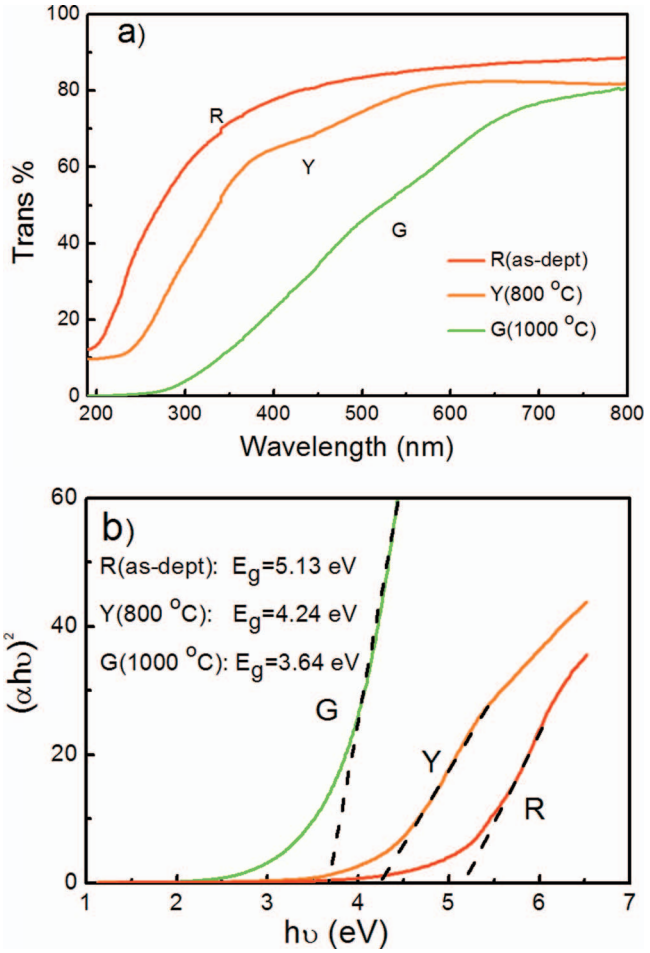

Figure 3. (a) Transmittance as a function of wavelength for LLZO thin films; (b) Plots of $(\alpha h\upsilon)^2$ as a function of photon energy ($h\upsilon$) for LLZO thin films.

shown in Figure 3a. These films were grown and annealed under the identical conditions as for the films on STO. XRD results showed that as-grown films were amorphous while films annealed at 800°C and 1000°C possessed cubic LLZO structure. As can be seen in Figure 3a, the overall transmittance of the annealed films is significantly lower in comparison to the as-deposited ones, possibly due to grain boundaries and defect development in the films.

As a candidate for lithium conductive electrolyte, it is important to study the film's bandgap E_g. E_g can be found out by extrapolating the linear portion of the absorption curve (Figure 3b) to the energy axis, according to the following equation:

$$\alpha = A(h\nu - E_g)^n / h\nu \quad [1]$$

where α is the absorption coefficient, A is a constant, and $n = \frac{1}{2}$ for direct bandgap and 2 for indirect bandgap materials.[16] The bandgap of the films was revealed to be direct corresponding to $n = \frac{1}{2}$. A band-gap value of 5.13 eV was estimated for the as-deposited LLZO films, which is larger than most electrochemical potential differences in lithium ion batteries. The films annealed at 800°C and 1000°C, exhibited lower bandgap values of 4.24 eV and 3.64 eV, respectively. Mechanism responsible for the lowering of the bandgap values for the annealed films is not very clear but we speculate, it may be related to increase in the crystallite size with higher annealing temperatures.

Au/LLZO/Pt cells were fabricated to examine the electrical properties of LLZO thin films. The Nyquist impedance of the as-deposited films, measured from 1 MHz to 100 Hz, is plotted as the black dots in Figure 4. The curve consists of a semicircle and a tail in the high and low frequency range, respectively. The data can

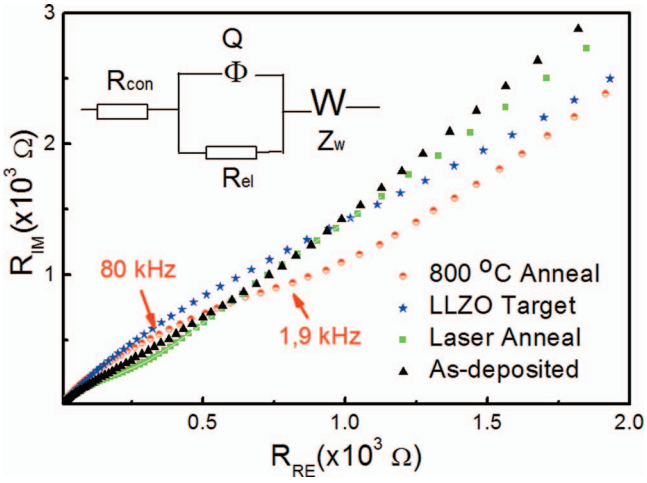

Figure 4. Nyquist impedance plots for LLZO films deposited and annealed at different conditions.

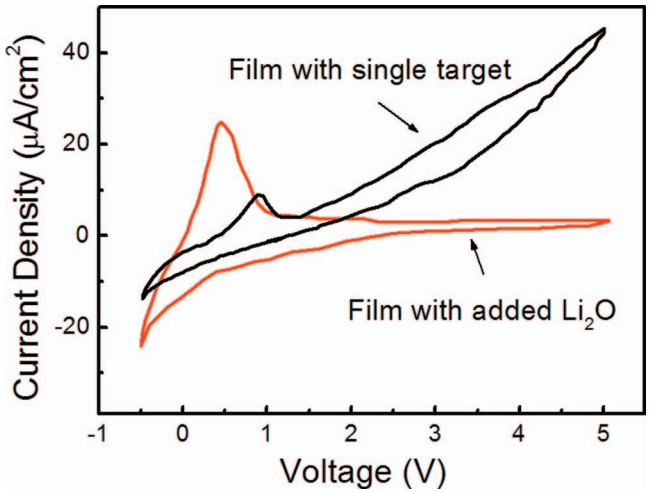

Figure 5. Cyclic voltammogram of the Li/LLZO/Pt cells made with the stoichiometric (i.e. prepared using LLZO and Li_2O targets) and the lithium deficient (i.e. prepared using only LLZO) LLZO films.

be fitted by an equivalent circuit shown in the inset, where R_{con} is the contact resistance, R_{el} is the electrolyte resistance, Q is the constant phase element, and Z_w is the Warburg impedance. By fitting the data to the equivalent circuit, while including dimensional parameters, we obtained an ionic conductivity value of 3.35×10^{-7} S/cm (R_{el}: 380 Ω) for the as-deposited films. This value is almost equal to the ionic conductivity of the tetragonal phase LLZO.[10] The activation energy for ion conduction was found to be 0.36 eV. The bulk and grain boundary resistance were not distinguishable in all of our films. The as-deposited films were amorphous; there was no grain boundary. The annealed films were crystalline; however, the films were very thin and the grain boundary wasn't even visible, therefore, the contribution from grain boundary was negligible. The ionic conductivity of the amorphous films is much less than that of the cubic LLZO, which may be attributed to the random arrangement of ions that impede the movement of lithium ions. The necessity of lithium compensation from an additional Li_2O target was also shown in Figure 4. As can be seen, by removing the Li_2O target, the as-deposited film possesses a much lower ionic conductivity of 7.19×10^{-8} S/cm (R_{el}: 1700 Ω), caused by lithium loss during deposition.

Influence of annealing on the ionic conductivity of the films was also studied, and the results are shown in Figure 4. After annealing the films at 800°C for 30 min, the ionic conductivity of the sample decreased to 1.78×10^{-7} S/cm (R_{el}: 720 Ω), almost half that of the as-deposited ones. This is possibly due to the larger resistance for ionic transport through the films that were full of defects and cracks. Therefore, high temperature annealing is not favorable for fast conduction of ions. Moreover, on further annealing at 1000°C, the platinum contact itself became oxidized and the cell showed a capacitor like behavior.

In order to enhance the ionic conductivity, the films were annealed using 25 ns pulses from a KrF excimer laser (248 nm wavelength). By shooting lasers, the film can crystallize very fast and possibly in a crack free way, since thermal expansion is a relatively slow process. Pulsed-laser annealing (PLA) was conducted by placing the film 1.5 feet away from the laser window. The intensity of the laser pulse was measured by an energy meter. Both the laser intensity and the number of pulses have been varied. According to our preliminary study, using 3 laser pulses of 1 J/cm^2 energy density, gave a well-crystallized film. The ionic conductivity of the annealed films was measured and shown in Figure 4. As can be seen, the semicircle of the spectroscopy for the PLA film is much smaller than the as-deposited one. Further calculation showed that the ionic conductivity increased to 7.36×10^{-7} S/cm (R_{el}: 180 Ω). The increase in ionic conductivity may result from the crystallization of LLZO in cubic phase. However, the conductivity value was orders of magnitude smaller than that of the cubic phase LLZO, which may be ascribed to the small size of the crystals which were formed only on the top of the films. To verify this, we have done XRD, SEM and optical transmittance tests on the PLA treated films. There was no peak in the XRD pattern, but we did see tiny grains (<100 nm) under SEM, and reduction of overall transmittance. These observations supported our speculation that only the very top layer of the film has been crystallized. For simplicity and clarity, the values of ionic conductivity and activation energy for those films are summarized in Table I. The variation of activation energy indicates the movement of lithium ions is easier in the lithium stoichiometric, crystalized smooth films.

The electrochemical stability of these two kinds of films (supplemented and not supplemented by lithium) was tested in Li/LLZO/Pt/STO cells. The film was firstly laser annealed, and then a thin piece of lithium metal was pressed on top of the film when sealing in a splitting cell. The cyclic voltammegrams of the Li/LLZO/Pt cells are shown in Figure 5. There're anodic and cathodic peaks around 0 V, which means the lithium ions can pass through the electrolyte and deposit on the Pt side and vice versa. The current at higher voltage vs. Li/Li^+ is quite small, indicating good stability of the stoichiometric film. However, the lithium deficient film is not quite stable at higher bias, as shown by the increasing current at high voltages. Therefore, the compensation of lithium during deposition indeed increases the electrochemical stability of the LLZO thin films.

Table I. Electrical properties of as-deposited film, thermal and laser annealed films and lithium deficient film.

Target	Annealing Condition (°C)	σ (S/cm)	Activation Energy (eV)
LLZO+Li_2O	As-deposited	3.35×10^{-7}	0.36
LLZO+Li_2O	800°C	1.78×10^{-7}	0.41
LLZO+Li_2O	Laser annealed	7.36×10^{-7}	0.32
LLZO	As-deposited	7.19×10^{-8}	0.45

Conclusions

We have successfully fabricated LLZO thin films through pulsed laser deposition at room temperature. The as-deposited films were amorphous and then were crystallized on annealing. The as-deposited films exhibited a good ionic conductivity of 3.35×10^{-7} S/cm at room temperature. Laser-annealing was found to increase the ionic conductivity of the film to the value of 7.36×10^{-7} S/cm. Moreover,

the electrochemical stability of the films against lithium metal was found to be quite satisfying. In summary, the LLZO represents a very promising solid-state electrolyte for the next generation thin-film batteries.

References

1. H. Chen, H. Tao, X. Zhao, and Q. Wu, *J. Non-Cryst Solids*, **357**, 3267 (2011).
2. J. K. Feng, L. Lu, and M. O. Lai, *J. J. Alloys Compd.*, **501**, 255 (2010).
3. J. E. Trevey, Y. S. Jung, and S. H. Lee, *Electrochimi. Acta*, **56**, 4243 (2011).
4. A. Sakuda and A. Hayashi, *J. Am. Ceram. Soc.*, **93**, 765 (2010).
5. W. R. Brant, S. Schmid, Q. Gu, R. L. Withers, J. Hester, and M. Avdeev, *J. Solid State chem.*, **183**, 1998 (2010).
6. A. Mei, X. L. Wang, J. L. Lan, Y. C. Feng, H. X. Geng, Y. H. Lin, and C. W. Nan, *Electrochimi. Acta*, **55**, 2958 (2010).
7. V. Thangadurai and W. Weppner, *J. Solid State chem.*, **179**, 974 (2006).
8. V. Thangadurai and W. Weppner, *Adv. Funct. Mater.*, **15**, 107 (2005).
9. R. Murugan, V. Thangadurai, and W. Weppner, *Angew. Chem. Int. Ed.*, **46**, 7778 (2007).
10. I. Kokal, M. Somer, P. H. L. Notten, and H. T. Hintzen, *Solid State Ionics*, **185**, 42 (2011).
11. M. Kotobuki, H. Munakata, K. Kanamura, Y. Sato, and T. Yoshida, *J. electrochem. Soc.*, **157**, A1076 (2010).
12. J. Tan and A. Tiwari, *Electrochem. Solid-State Lett.*, **15**, A37 (2012).
13. H. Buschmann, S. Berendts, B. Mogwitz, and J. Janek, *J. Power Sources*, **206**, 236 (2012).
14. R. Murugan, S. Ramakumar, and N. Janani, *Electrochim. Commun.*, **13**, 1373 (2011).
15. H. Buschmann, J. Dölle, S. Berendts, A. Kuhn, P. Bottke, M. Wilkening, P. Heitjans, A. Senyshyn, H. Ehrenberg, A. Lotnyk, V. Duppel, L. Kienle, and J. Janek, *Phys. Chem. Chem. Phys.*, **13**, 19378 (2011).
16. F. I. Ezema and R. U. Osuji, *Chalcogenide Lett.*, **13**, 1373 (2011).